nature communications

Article

https://doi.org/10.1038/s41467-025-63254-z

Post-functionalization of polyethers by photoinduced C–H amidation via polar-radical relay

Received: 7 February 2025

Accepted: 14 August 2025

Published online: 26 August 2025

Check for updates

Seung Beom Baek[1,2,5], Youngho Kim[1,5], Wongyu Lee[1,2], Sangwon Seo[2,3], Dongwook Kim[1,2], Myungeun Seo[1,4] ✉ & Sukbok Chang[1,2] ✉

The C–H functionalization of polymers enables the direct incorporation of new functional groups into polymer backbones, presenting significant opportunities for the upcycling of commodity polymers. However, developing reactions that achieve selective functionalization while preserving the intrinsic features of polymers and avoiding undesirable structure deformation remains a considerable challenge. In this study, we present a transition metal-free post-functionalization approach for polyethers via a photoinduced α-C–H amidation reaction. This strategy provides a route to previously unattainable α-amino polyethers, which exhibit distinct physical properties from those of the parent polymer. By leveraging a polar-radical relay mechanism, we effectively incorporate C–N bonds into the polyether backbone while suppressing degradation and cross-linking. Conducted under mild and convenient conditions, this approach demonstrates significant site selectivity at the ethereal α-position, even in the presence of other types of C–H bonds, achieving tailed post-functionalization of macromolecules. Furthermore, the present strategy holds promise for broader applications, including the amidative degradation of commodity polymers and transformation of polyethylene glycol (PEG) network.

The utilities of polymers are heavily dependent on properties such as rigidity, solubility, or interfacial tension. These unique characteristics can be controlled by incorporating or modifying pendent functional groups attached to the polymer backbone[1–3]. Over the past few decades, various polymerization methods have been explored, enabling the selective introduction of certain functional groups, aimed to produce customized polymers having desired properties. However, practical issues often arise in polymer synthesis, representatively the incompatibility of functional monomers with conventional polymerization processes. For example, polar-functional group bearing comonomers may cause catalyst poisoning, restricting the range of accessible functionalized polymers[4,5].

A promising alternative approach to obtaining functionalized polymers is the post-modification of readily accessible polymers[3,6]. In this context, desirable functional groups can be introduced through C–H functionalization starting from commodity polymers, without the need for prior transformation of the parent polymers[7–9] (Fig. 1a). This approach has been successfully demonstrated in the post-polymerization modification (PPM) of various polymers, including polyethylene (PE)[10,11], polypropylene (PP)[12,13], polystyrene (PS)[14,15] polyethylene oxide (PEO), and polyethylene glycol (PEG)[16–18]. Thus, newly modified polymers often exhibit unique properties that are difficult to access through the conventional polymerization methods[6]. Although highly efficient and advanced C–H transformations are well

[1]Department of Chemistry, Korea Advanced Institute of Science and Technology (KAIST), Daejeon, South Korea. [2]Center for Catalytic Hydrocarbon Functionalizations, Institute for Basic Science (IBS), Daejeon, South Korea. [3]Department of Physics and Chemistry, Daegu Gyeongbuk Institute of Science and Technology (DGIST), Daegu, South Korea. [4]KAIST Institute for the Nanocentury, KAIST, Daejeon, South Korea. [5]These authors contributed equally: Seung Beom Baek, Youngho Kim. ✉e-mail: seomyungeun@kaist.ac.kr; sbchang@kaist.ac.kr

https://doi.org/10.1038/s41467-025-63254-z

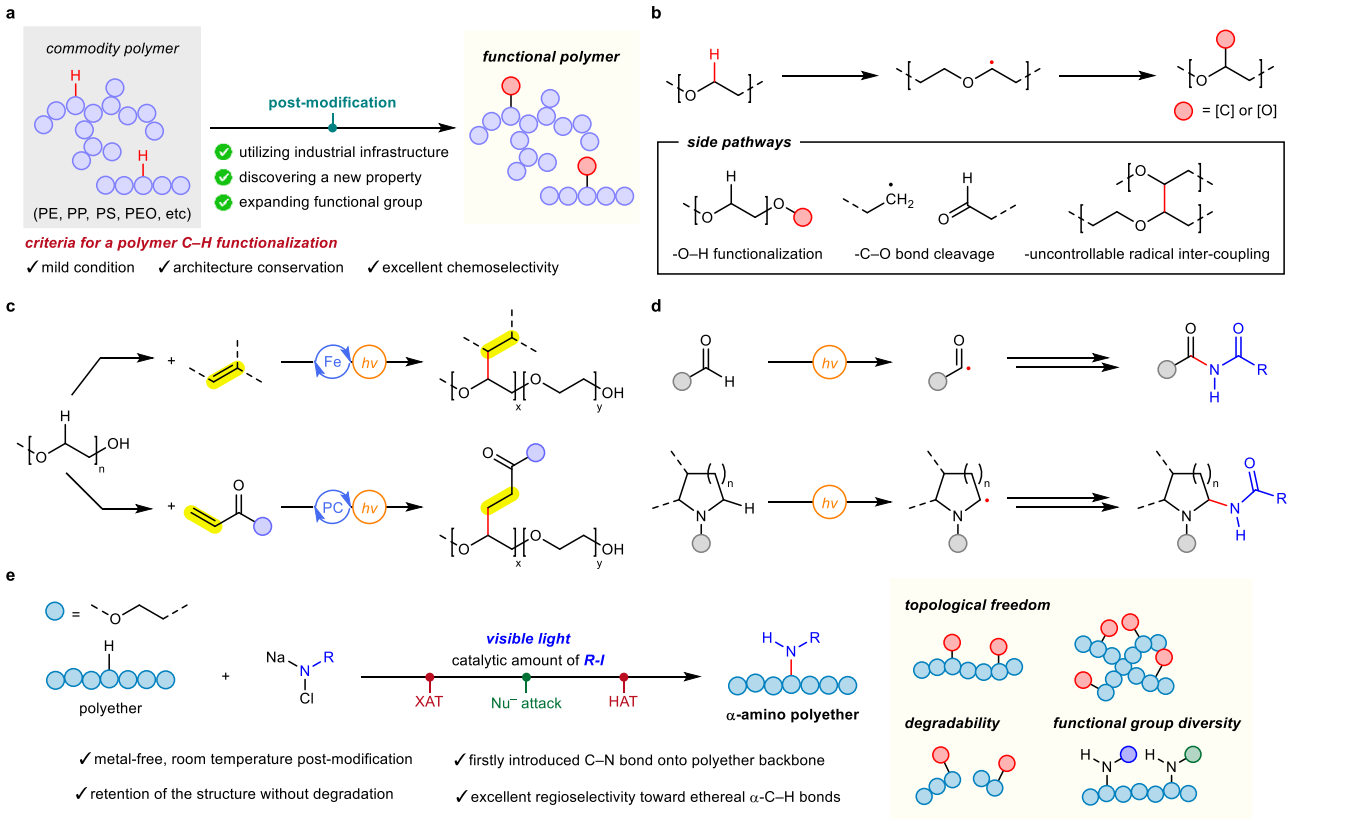

Fig. 1 | Concept of polymer post-modification and description of present work. **a** C–H functionalization of commodity polymers. **b** Post-modification of polyethers. **c** Examples for C–H alkylation of PEGs suppressing degradation. **d** Previous works for photoinduced metal-free amidation of aldehydes and cyclic amines. **e** This work: α-amidation of ethers enabling polyether post-modification.

established for small molecules[19,20], achieving advanced level of polymer C–H functionalization requires additional careful considerations[9]. Mild reaction conditions are necessary for the upcycling while minimizing changes to the polymer architecture, and PPM should ensure high chemoselectivity for the targeting functionalization, as separating multiple functional groups is not feasible after incorporation of functional groups onto single polymer chain.

Polyethylene glycol (PEG) is a prominent member of polyether subclass, well-known for its biocompatibility[21–23], application in hydrogel synthesis,[24] and ion-conducting properties[25–28]. Given that commercial PEGs generally have reactive hydroxyl groups at both ends, their chain-end functionalization is common[29–31], whereas the aliphatic C–H modification has been contrarily limited (Fig. 1b). Although independent studies by Parent[32], Elisseeff[33] and Bielawski[34] groups have reported the incorporation of C–C or C–O bonds into PEG derivatives, these approaches are often accompanied with polymer degradation.

Recently, Zeng et al. demonstrated an α-C–H alkylation of polyethers with minimal polymer degradation[16,17] (Fig. 1c), where photoinduced C–H bond cleavage enables subsequent C–C bond formation in reaction with electron-deficient alkenes, using iron or iridium catalysis under blue LED irradiation. However, synthetic approaches for introducing heteroatoms into the polyether backbone without degradation remain largely underdeveloped. Although α-amination of small ether molecules is well established in synthetic chemistry[35], utilizing practical N-sources such as oxycarbamates[36,37], azides[38,39] or dioxazolones[40], either through transition metal-catalyzed or metal-free oxidative conditions, extending this approach to polymer substrates remains a significant challenge.

In our ongoing research program to develop C–N bond formation methods, we recently reported the visible light-induced C–H amidation of aldehydes and cyclic amines[41,42] (Fig. 1d). The reaction was proposed to proceed via the cleavage of sp^2- or sp^3-C–H bonds through hydrogen atom transfer (HAT), following controlled relay of carbon radical intermediates. The mild conditions combined with practical amidation reagents prompted us to explore the potential for extending this strategy into polymers[43–45]. Herein, we describe our new development of a photoinduced regio- and chemoselective α-amidation of polyethers under metal-free, visible light irradiation conditions, using a catalytic amount of alkyl iodide as an initiator (Fig. 1e). Current transformation was found to occur via a polar-radical relay pathway, which consists of HAT, halogen atom transfer (XAT), nucleophilic attack by the amino reagent, and then re-starting of the cycle by subsequent HAT. It represents the first example of introducing C–N bonds directly onto the polyether backbone to suppress the degradation of main chain, thereby making α-amino polyethers, previously inaccessible through co-polymerization[30,46,47]. Excellent site selectivity toward ethereal α-position leads to regioselective amidation of polyether derivatives including block-copolymers, even possessing benzylic C–H or ester groups. Additionally, further applications of present strategy, such as PPM of PEG network or introducing degradable features to macromolecules, were demonstrated.

Results

Reaction development

We began our study by investigating the α-C–H amidation of tetrahydrofuran (THF) **1a** as a model substrate, reacting it with readily accessible and bench-stable *N*-chloro-*N*-sodio-*tert*-butylcarbamate **2a**[43–45] under various conditions (Fig. 2a). We hypothesized that the postulated polar-radical relay process would commence with the activation of an ethereal α-C–H bond, leading to the formation of an *N*-

https://doi.org/10.1038/s41467-025-63254-z

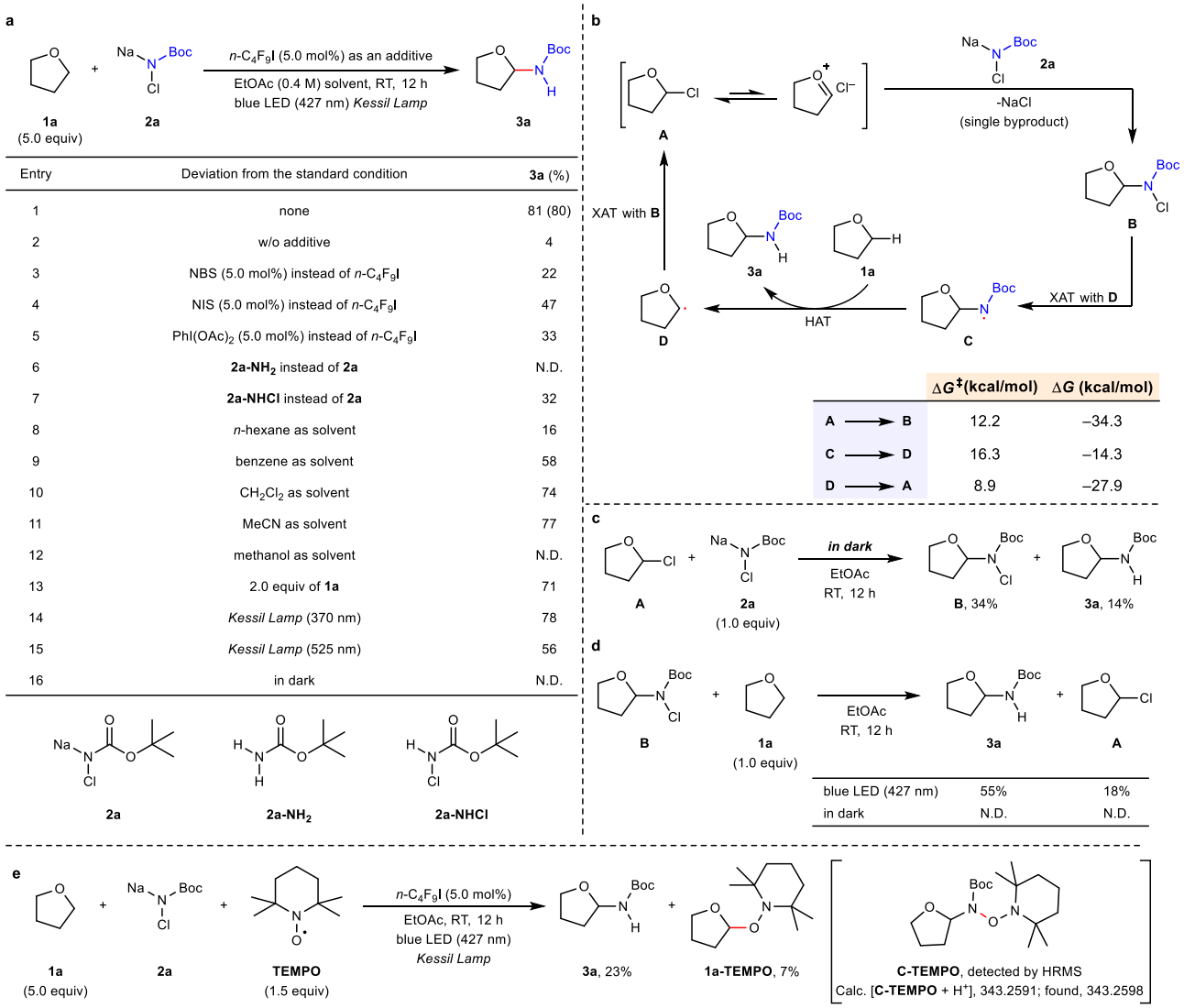

Entry	Deviation from the standard condition	3a (%)
1	none	81 (80)
2	w/o additive	4
3	NBS (5.0 mol%) instead of *n*-C_4F_9I	22
4	NIS (5.0 mol%) instead of *n*-C_4F_9I	47
5	$PhI(OAc)_2$ (5.0 mol%) instead of *n*-C_4F_9I	33
6	**2a-NH$_2$** instead of **2a**	N.D.
7	**2a-NHCl** instead of **2a**	32
8	*n*-hexane as solvent	16
9	benzene as solvent	58
10	CH_2Cl_2 as solvent	74
11	MeCN as solvent	77
12	methanol as solvent	N.D.
13	2.0 equiv of **1a**	71
14	*Kessil Lamp* (370 nm)	78
15	*Kessil Lamp* (525 nm)	56
16	in dark	N.D.

2a **2a-NH$_2$** **2a-NHCl**

Fig. 2 | Optimization & proposed mechanism for polar-radical relay. **a** Optimization table: Reactions were carried out on 0.2 mmol scale in EtOAc. Yields were determined by ^{1}H NMR spectroscopy of the crude reaction mixture using 1,1,2-trichloroethane (1,1,2-TCE) as an internal standard. Isolate yields are given in parentheses. N.D. not detected. **b** Proposed pathway of polar-radical relay process. **c** Mechanistic experiment for nucleophilic C–N bond formation between 2-chlorotetrahydrofuran and **2a**. **d** HAT & XAT experiments between *N*-chlorohemiaminal and **1a**. **e** Radical trapping experiment using 2,2,6,6-tetramethylpiperidinyloxy (TEMPO).

chlorohemiaminal intermediate[42]. Since fluoroalkyl iodides are known to readily generate alkyl radicals under photoirradiation[48–52], we explored their potential role as initiators in this amidation to see whether they could promote the desired hydrogen atom abstraction at the α-C–H bonds of ether substrates[51,52].

When the reaction was performed under 427 nm irradiation in ethyl acetate (EtOAc) as the solvent, the targeted α-amino ether product **3a** was obtained from THF (5.0 equiv) in 80% isolated yield in the presence of *n*-C_4F_9I (5.0 mol%, Fig. 2a, entry 1). However, the amidation did not take place to a noticeable level in the absence of this additive (Fig. 2a, entry 2). On the other hand, the addition of *N*-halosuccinimides or $PhI(OAc)_2$, well known as oxidants for ether or amine[42,53,54], induced the reaction only moderately (Fig. 2a, entries 3–5). Using *tert*-butyl carbamate (**2a-NH$_2$**) as an alternative amidating reagent was completely ineffective (Fig. 2a, entry 6), but its *N*-chloro derivative **2a-NHCl** furnished the amidated product **3a** in 32% yield (Fig. 2a, entry 7). The reaction efficiency was found to be sensitive to solvents (Fig. 2a, entries 8–12), showing that higher product yields were obtained in polar non-protic media such as ethyl acetate, methylene chloride or acetonitrile. Satisfactory amidation efficiency was achieved even with 2.0 equiv of THF relative to the amidating reagent **2a** (Fig. 2a, entry 13). The amidation efficiency remained almost consistent with UV-region irradiation (Fig. 2a, entry 14), and slightly decreased with long-wavelength (Fig. 2a, entry 15), but no reaction occurred in dark (Fig. 2a, entry 16).

Building on our previous reports[41,42], a plausible mechanistic pathway for the photoinduced α-C–H amidation is illustrated in Fig. 2b. The postulated relay process begins with the formation of an α-chloro ether intermediate **A**, which reacts with the amidating reagent, *N*-chloro-*N*-sodio-*tert*-butylcarbamate **2a**, to afford photoresponsive hemiaminal **B**. Under photoirradiation, this intermediate undergoes a homolytic cleavage to give rise to amidyl (**C**) and chloride radicals. Hydrogen atom transfer (HAT) between the α-C–H bond of the starting material THF and N-centered radical **C** yields the desired α-amino ether **3a** along with a carbo radical species **D**. A subsequent halogen atom transfer (XAT) of this intermediate with N–Cl bond of **B**, or radical recombination with chloride radical, regenerates the α-chloro ether compound **A**. Density functional theory (DFT) calculations on the C–N bond formation, hydrogen atom abstraction and radical intermediate

captivation step support the viability of the proposed relay cycle (Fig. 2b, bottom right).

To shed light on the mechanistic aspects, we performed a series of probe experiments (Fig. 2c, d). The reaction between the α-chloro ether intermediate **A** with the amidating reagent **2a** proceeded in the dark, albeit in moderate efficiency, consistent with the proposed mechanism (Fig. 2c). When a mixture of *N*-chlorohemiaminal **B** and THF (**1a**) was irradiated with blue LED, the protonated hemiaminal (**3a**) was formed in 55% yield, along with 2-chlorotetrahydrofuran (**A**) in 18% (Fig. 2d). In stark contrast, formation of **A** was not observed in the absence of light, highlighting the critical role of photoirradiation in this radical replay process. When the amidation was conducted in the presence of 2,2,6,6-tetramethylpiperidinyloxy (TEMPO), a well-known radical scavenger[55], the reaction efficiency significantly decreased, and a THF-TEMPO adduct (**1a-TEMPO**) was detected (Fig. 2e). Furthermore, an amidyl-TEMPO adduct (**C-TEMPO)** was observed via mass spectrometry, providing evidence for the formation of the N-centered radical **C** as postulated in Fig. 2b.

Substrate scope

With the optimal photoinduced amidation conditions established, we subsequently investigated the reaction scope across various ether substrates (Fig. 3). First, a range of practical amidating reagent, primary carbamates or sulfonamide in their *N*-chloro-*N*-sodio form, were effectively utilized for site-selective amidation of THF under the photoirradiation protocol. It should be mentioned that these bench-stable amidating reagents can be conveniently prepared from their corresponding carbamates or sulfonamide in two high-yielding steps: oxidation with trichloroisocyanuric acid (TCCA) followed by treatment with NaOH[41–43,56]. These reagents featuring Boc- (**2a**), Cbz- (**2b**), Troc- (**2c**) and Tosyl- (**2d**) groups were successfully employed, yielding ether products (**3a**–**3d**) in moderate to good yields. Cyclic ethers, such as tetrahydropyran and 1,4-dioxane, underwent selective α-position amidation, furnishing the corresponding products **3e** and **3f**, respectively, in good yields under slightly modified conditions. An Ambroxide-derived substrate was efficiently amidated at its α-C–H bond, yielding product **3g**. Benzo-fused cyclic ethers were examined using *N*-iodosuccinimide (NIS) as an additive, achieving high regioselectivity and good yields (**3h** and **3i**). Notably, amidation occurred selectively at the benzylic ethereal α-carbon without affecting the carbo benzylic position (**3h**).

Amidation was found to be more preferred at the benzylic ethereal α-C–H bonds and potentially reactive non-benzylic counterparts remained intact (**3j**–**3n**), thus demonstrating that the present photoinduced amidation is highly regio- and chemoselective. Interestingly, alkyl bromide and epoxide groups were compatible with the optimal conditions (**3k** and **3l**). An ether derivative of Menthol was successfully amidated at the ethereal benzylic C–H bonds using Troc- amidating reagent (**3n**). Acyclic aliphatic ethers, representatively diethyl ether, also smoothly underwent regioselective amidation with several amidating reagents (**3o**–**3q**). Notably, the reaction efficiency for dibutyl ether was not significantly affected when it was employed in an equimolar ratio (1:1) relative to the amidating reagent, achieving good product yield (**3r**). Primary ethereal α-C–H bond also yielded hemiaminal product under the optimal conditions (**3s**). As demonstrated by a reaction of 2-phenylethyl methyl ether (**1t**), the amidation was favored at the secondary ethereal α-C–H bonds over the primary methyl counterpart (**3ta** and **3tb**), while the benzylic C–H bonds were intact. Ester functional group was compatible with the current photoirradiation protocol, and the amidation occurred exclusively at the two viable α-ethereal C–H bonds (**3ua** and **3ub**), without reacting at the alkoxy moiety of ester. When two reacting sites are sterically differed, the amidation was favored at the secondary over the tertiary C–H bonds (**3v**), still showing high compatibility to the ester group. In addition, when a crown ether (12-crown-4) was subjected to photoinduced conditions, amidation was observed albeit with moderate yield (**3w**), demonstrating the potential of applying this method to polyether macromolecules.

Post-polymerization amidation

Building on the successful photoinduced selective amidation of small molecular ethers, we next investigated its potential as a tool for the post-modification of polymers. Applying organic reaction conditions to macromolecules introduces several challenges as the inherent robustness of polymers often alters reactivity observed in small-molecule systems[9]. In particular, C–H functionalization of polymers demands careful considerations of the unique properties of macromolecules, both in the starting materials and in the functionalized products, often necessitating new reaction optimizations. Encouragingly, our photoinduced α-amidation procedure for small ether molecules could be successfully applied to the polyether post-modification without significant alternations (Fig. 4). As a model substrate, we selected poly(ethylene glycol) (PEG) with a number-average molar mass (M_n) of 4600 g/mol, containing ~104 ethylene oxide (EO) repeating units per chain and hydroxyl groups at both terminals. When the polymer was treated with 20.0 mol% of the amidating reagent **2a** (relative to the number of repeating units) under blue light irradiation, ^{1}H NMR analysis confirmed the incorporation of an amino group at the ethereal α-position (Fig. 4a). Notably, the reaction proceeded efficiently at room temperature in the eco-friendly solvent (EtOAc)[57] without the need for metal catalysts, thereby allowing us to synthesize a new class of polymer, α-amino polyether, for the first time.

We next measured the level of functionalization (LOF) as the molar fraction of functionalized EO repeating units. Initially, the LOF increased gradually, then accelerated rapidly, eventually reaching a plateau at ~10 mol% after 90 min (Fig. 4b). This sharp change in rate was attributed mainly to the hydrogen atom transfer (HAT) step, which involves different radical species (i.e., C_4F_9 or amidyl radical). Notably, the weight-average molar mass (M_w) of the functionalized PEG, estimated via size exclusion chromatography (SEC), showed a slight increase over time. This suggests that polymer substrate degradation through chain scission was effectively suppressed in the present polar-radical relay process. Furthermore, the SEC traces indicate a shift towards higher molar mass due to functionalization, without significant broadening of the molar mass distribution (Fig. 4c). This highlights the rarity of such results in aliphatic C–H PPM of polyethers without significant chain scission. The growing presence of lower molar mass fraction is likely due to unfunctionalized PEG chains, stemming from the stochastic nature of the reaction.

Significantly, the LOF increased linearly with the amount of amidating reagent **2a**, demonstrating precise control over the degree of functionalization (Fig. 4d). Highly functionalized PEGs were successfully obtained, with up to 20 mol% incorporation of amino groups per repeating unit. Moreover, the M_n and polydispersity index (PDI) values indicated that no significant chain scission occurred under the current reaction conditions. However, when the loading of amidating reagent **2a** exceeded 60.0 mol%, the amidation efficiency declined, resulting in saturation of the LOF and degradation of the PEG backbone (see Supplementary Figs. 14, 16). Under diluted conditions, complete decomposition of the polymer backbone was observed upon addition of 100.0 mol% of the amidating reagent (see Supplementary Fig. 17). This undesired chain scission is likely attributable to the increased formation of highly reactive intermediates, such as ethereal α-carbon radicals, as well as the intrinsic instability of the hemiaminal moiety.

The reaction was efficiently scalable, allowing for the production of amidated PEGs with varying LOF values in multi-gram quantities (See Supplementary Figs. 18, 19). As expected, amidation on the main chain of the PEG, remarkably altered its physical properties. While the parent PEG is a semicrystalline white powder at room temperature, amidation resulted in a yellow coloration. When amide loading

https://doi.org/10.1038/s41467-025-63254-z

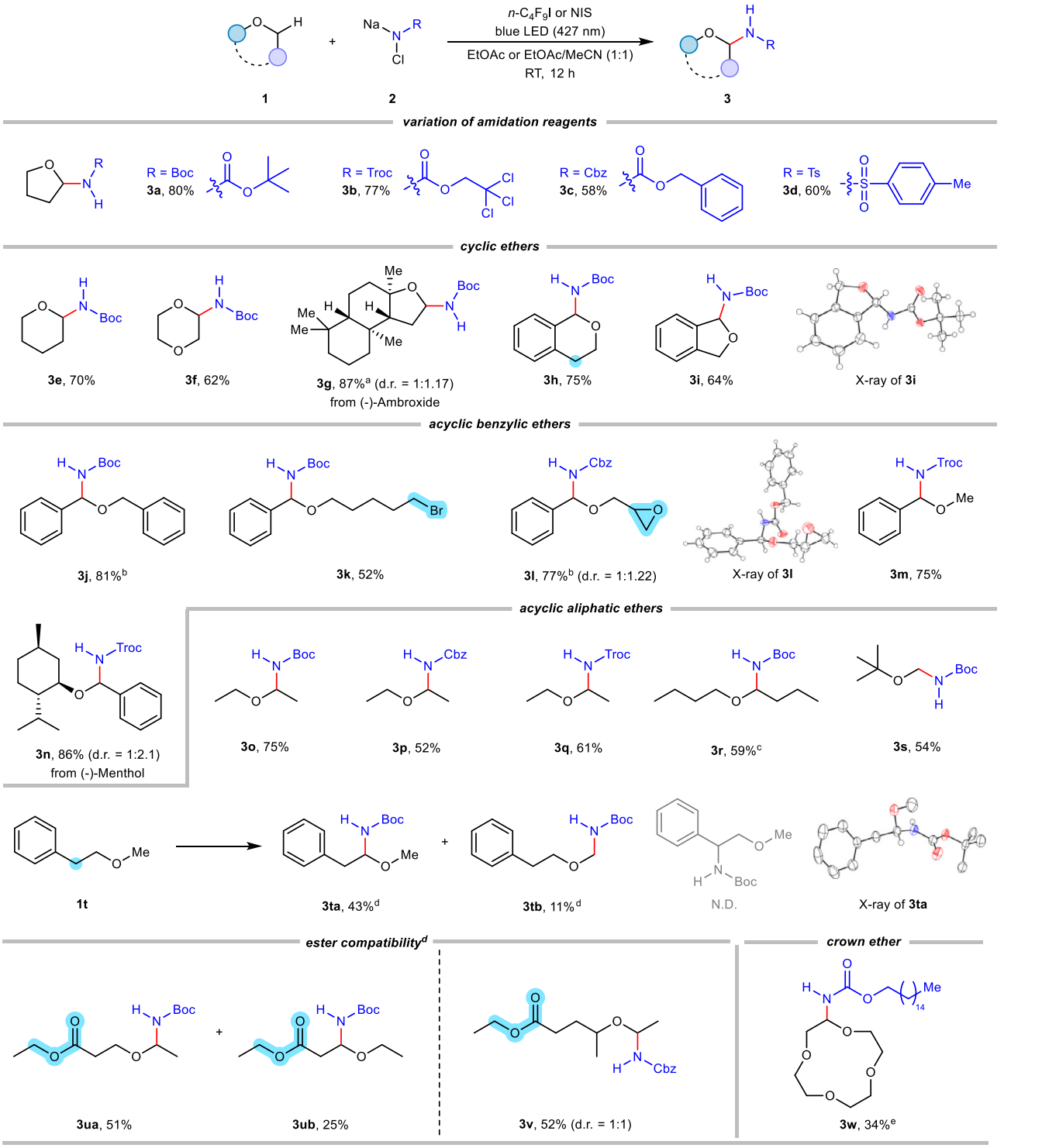

Fig. 3 | Substrate scope of ethers. Reactions were carried out under N_2 atmosphere using amidating reagent (0.2 mmol), ether (1.0 mmol), *n*-C_4F_9I (5.0 mol%), blue LED (427 nm, Kessil Lamps) and EtOAc at RT for 12 h. For 6-membered cyclic ethers, MeCN/EtOAc (1:1) was applied, using 10.0 equiv of ether and 20.0 mol% of *n*-C_4F_9I. For benzo-fused or benzylic ethers, EtOAc was applied, using 1.2 equiv of *N*-chloro-*N*-sodio-carbamate (based on 1.0 equiv of ether) and 2.0 mol% of NIS instead of *n*-C_4F_9I. [a]2.0 Equiv of ether was used. [b]*N*-Chloro-*N*-sodio-carbamate (0.2 mmol), ether (0.4 mmol), and *n*-C_4F_9I (5.0 mol%) were used. [c]1.0 Equiv of ether was used. [d]10.0 mol% of *n*-C_4F_9I was used. [e]1.2 Equiv of ether was used.

exceeded 5 mol%, the amidated polymer became a dark yellow liquid, suggesting that the amino functionality may disturb the crystalline packing of the PEG chains.

The visual change in physical properties prompted us to measure the thermal transitions of the α-amino PEG products with varying degrees of the amide group functionalization using differential scanning calorimetry (DSC, Fig. 4e, f). As with most polymers, the thermal properties of polyethers play a critical role in their material science applications, such as solid-state electrolytes. Investigating the correlation between ionic conductivity and thermal properties, including the glass transition temperature (T_g), is a key area of research[58,59]. At functionalization levels below 3 mol% of LOF, a gradual

https://doi.org/10.1038/s41467-025-63254-z

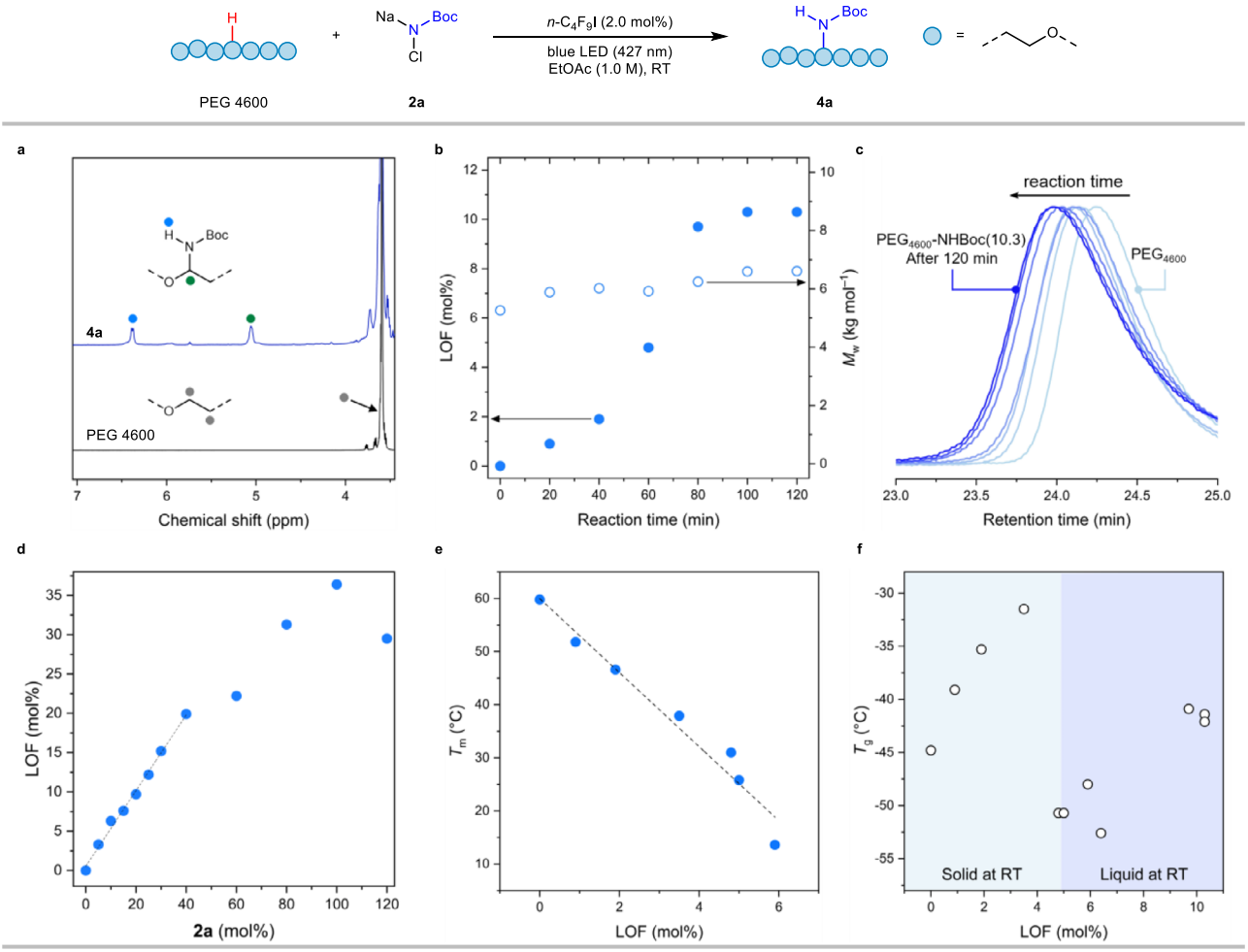

Fig. 4 | α-Amidation of polyethers by polar-radical relay process. a ^{1}H NMR spectroscopy for PEG 4600 ($CDCl_3$) and **4a** ($(CD_3)_2CO$). **b** Change of LOF and M_w varying reaction time (20 mol% of **2a** was used). **c** SEC traces (THF as an eluent) of **4a** varying reaction time (20 mol% of **2a** was used). **d** LOF changes of α-amidation versus the amount of **2a**. **e** T_m of **4a** with different LOFs. **f** T_g of **4a** with different LOFs.

decrease in melting temperature (T_m) was observed alongside an increase in T_g. This behavior can be attributed to disrupted chain packing and increased interchain interactions due to the polar amino group. At around 5 mol% of LOF, PEG failed to crystalize when cooled to −80 °C, and the glass transition occurred at lower temperatures (<−50 °C). At higher amino content, crystallinity still decreased, resulting in rubbery materials with T_g of around −40 °C. Overall, the thermal transitions were significantly affected by small amounts of amide group incorporation. These findings highlight the potential to finely tune the thermal properties of polyethers through amide group functionalization, suggesting a promising application in polymer electrolytes, as PEG crystallinity is known to hinder ion mobility below T_m[60].

Substrate scope of polyethers

We next explored the potential of the current photoinduced α-amidation of polyether derivatives (Fig. 5). Significantly, the reaction proceeded smoothly across a range of PEGs, irrespective of their molar masses. Polymers with M_n ranging from 2,000 to 1,000,000 g/mol were successfully amidated under optimal conditions, achieving consistent LOF values between 4.2–5.6 mol% (**4a**–**4e**). After completion of the reaction, the crude polymers were purified by precipitation, and some were further subjected to dialysis to remove residual small-molecule byproducts (See Supplementary Information for details). While the molar mass dispersity ($Đ$) of the functionalized polymers was comparable to the parent polymers in most cases, we observed broadening of molar mass distributions especially for higher-molar mass reactants, suggesting the increase of interaction between the product and SEC column, or chain coupling. The tolerance for a wide range of molecular weights underscores the high potential of this PPM for PEGs with various applications, from plasticizers to binder[61].

Variations in polymer architectures, such as methoxy-terminated chains (**4f**, 4.5 mol%) and star-shaped PEG structures with four "arms" (**4g**, 5.3 mol%), did not affect the reaction efficiency. The increased PDI value observed for **4g** may be attributed to a higher likelihood of chain coupling, due to its star-shaped backbone structure. PEG could also be functionalized with other carbamate reagents bearing -NHCbz (**4h**, 5.2 mol%) or -NHTroc (**4i**, 5.0 mol%), consistent with results observed in small molecule reactions. Furthermore, an isotope-labeled amide group could be successfully incorporated (**4b-^{15}N**, 4.7 mol%) through reaction with 10 mol% of **2a-^{15}N**. Since PEG materials are widely used in bioactive applications, synthesized **4b-^{15}N** holds potential for use in metabolic studies or bio-imaging[62]. Polytetrahydrofuran (PTHF), composed of butylene oxide repeating units, was also successfully converted into its α-amino derivative without amidation occurring at the other remote C–H bonds (**4j**).

Since the current amidation occurs selectively at the ethereal α-C–H bonds, we envisioned extending this photoinduced radical approach even to block copolymers containing polyether segments.

https://doi.org/10.1038/s41467-025-63254-z

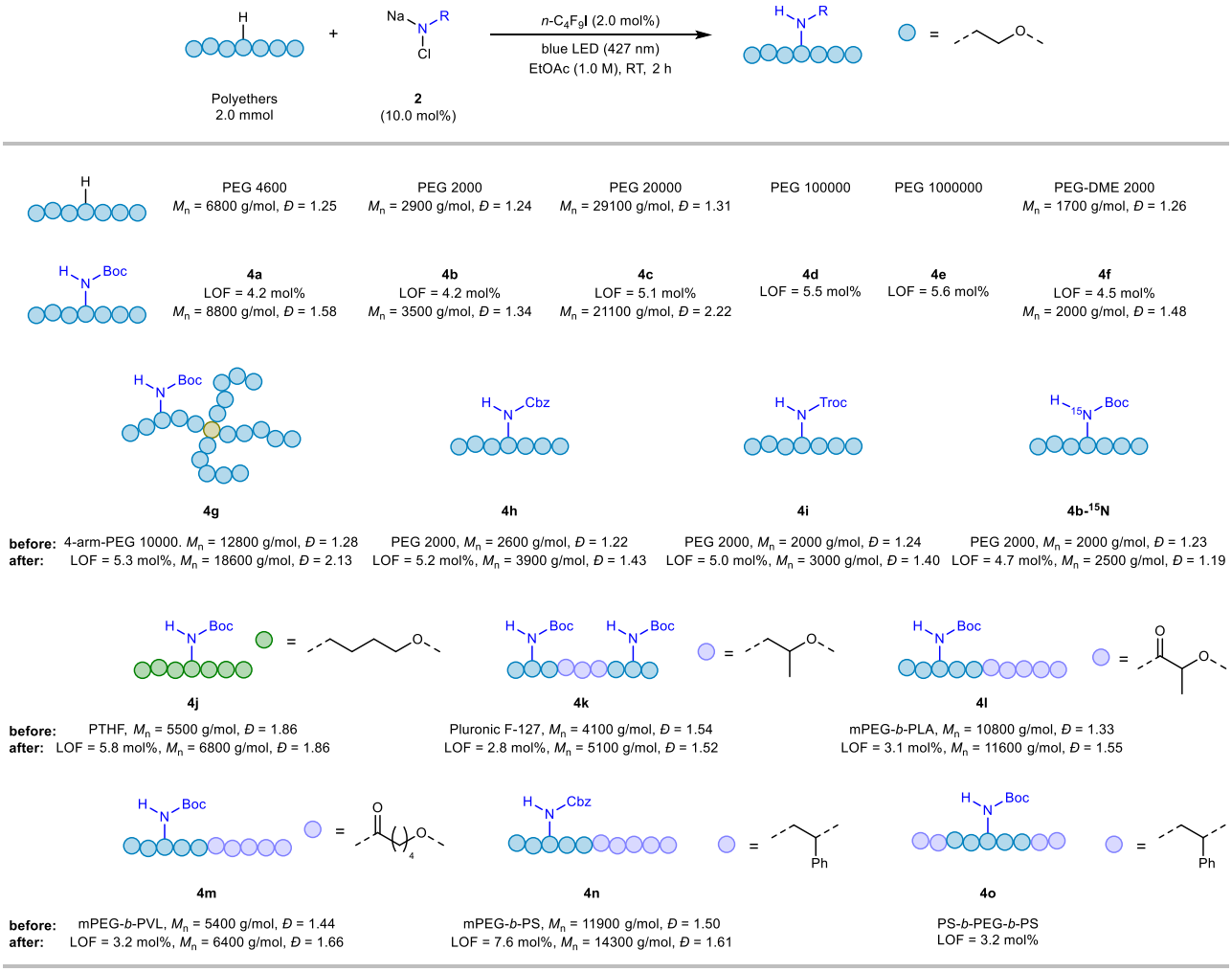

Fig. 5 | Scope of polyether functionalization. Reactions were carried out under N_2 atmosphere using polyethers (2.0 mmol scale of repeating unit), *N*-chloro-*N*-sodio-carbamate (10.0 mol%), *n*-C_4F_9I (2.0 mol%), blue LED (427 nm, Kessil Lamps) and EtOAc (2.0 mL) at RT for 2 h. LOFs were determined by ^1H NMR, relative to unmodified repeating unit. M_n were determined by SEC analyses using DMF/LiBr as an eluent.

Block copolymers are widely used in materials science[63], for example, in the formation of micelles[64,65] or self-assembly structures[66–68]. In fact, PEG-polylactide (PEG-PLA) block copolymers are known to serve as carriers for small molecules[69,70]. Despite their promising applications, site-selective post-functionalization of block copolymers remains challenging, as the incorporation of functional groups often fails to distinguish between different blocks due to their competing reactivities or harsh reaction conditions. In our study, amidation on Pluronic triblock copolymers occurred selectively at the ethylene oxide site in the PEG end blocks, while the tertiary ethereal α-C–H bond in the poly(propylene oxide) (PPO) midblock remained unaffected (**4k**). Likewise, C–H bonds in polyesters such as PLA and polyvalerolactone (PVL), as well as benzylic C–H bonds in polystyrene (PS), were inactive, resulting in selective amidation of the PEG block (**4l**–**4n**). Similarly, treatment of a PS-*b*-PEG-*b*-PS triblock copolymer with the amidating reagent **2a** provided a rubbery PEG midblock reinforced by PS hard segments (**4o**).

Material applications

To explore the potential for expanding the synthetic utility of the current post-polymerization approach, several transformations were additionally examined (Fig. 6). As shown in the -NHCbz and -NHTroc installation (**4h** and **4i**), various functional groups can be immobilized on the polyether backbone using different carbamates. We further show that several urethane-functionalized PEGs can be readily obtained (Fig. 6a, above). In addition to the long alkyl pendant, potentially rendering hydrophobicity (**4p**), we found that chemical handles such as alkyne (**4q**) for further modification can be included and stay intact during the amidation. Moreover, we investigated the photoinduced amidation starting from either free carbamate or amide, via in situ preparation of *N*-chloro-*N*-sodio-carbamate (Fig. 6a, below). By treating the amide with TCCA, corresponding *N*-chloroamide could be easily prepared. Without the need for chromatography or recrystallization, the *N*-chloroamides were directly used in PPM, followed by the addition of sodium hydroxide (NaOH) to form the *N*-salt in the reaction mixture. Under photoirradiation, functional groups such as trimethylsilylethyl carbamate or deuterated acetamide were successfully incorporated onto the polyether backbone (**4r** and **4s**). This practical amidation method, capable of introducing various functional groups even starting from primary amide moieties, highlights the potential of the current strategy for customizing the physical and chemical properties of polyether derivatives.

Next, we discovered that the incorporation of two different carbamates into a single PEG chain was also achievable in a single reaction. By adding 10.0 mol% of each aminating reagent **2a** and **2b** to a solution of PEG 4600, we successfully obtained functionalized polyethers bearing 2.6 mol% of -NHBoc and 3.2 mol% of -NHCbz groups simultaneously (Fig. 6b). While the functionalized polyethers are stable in

https://doi.org/10.1038/s41467-025-63254-z

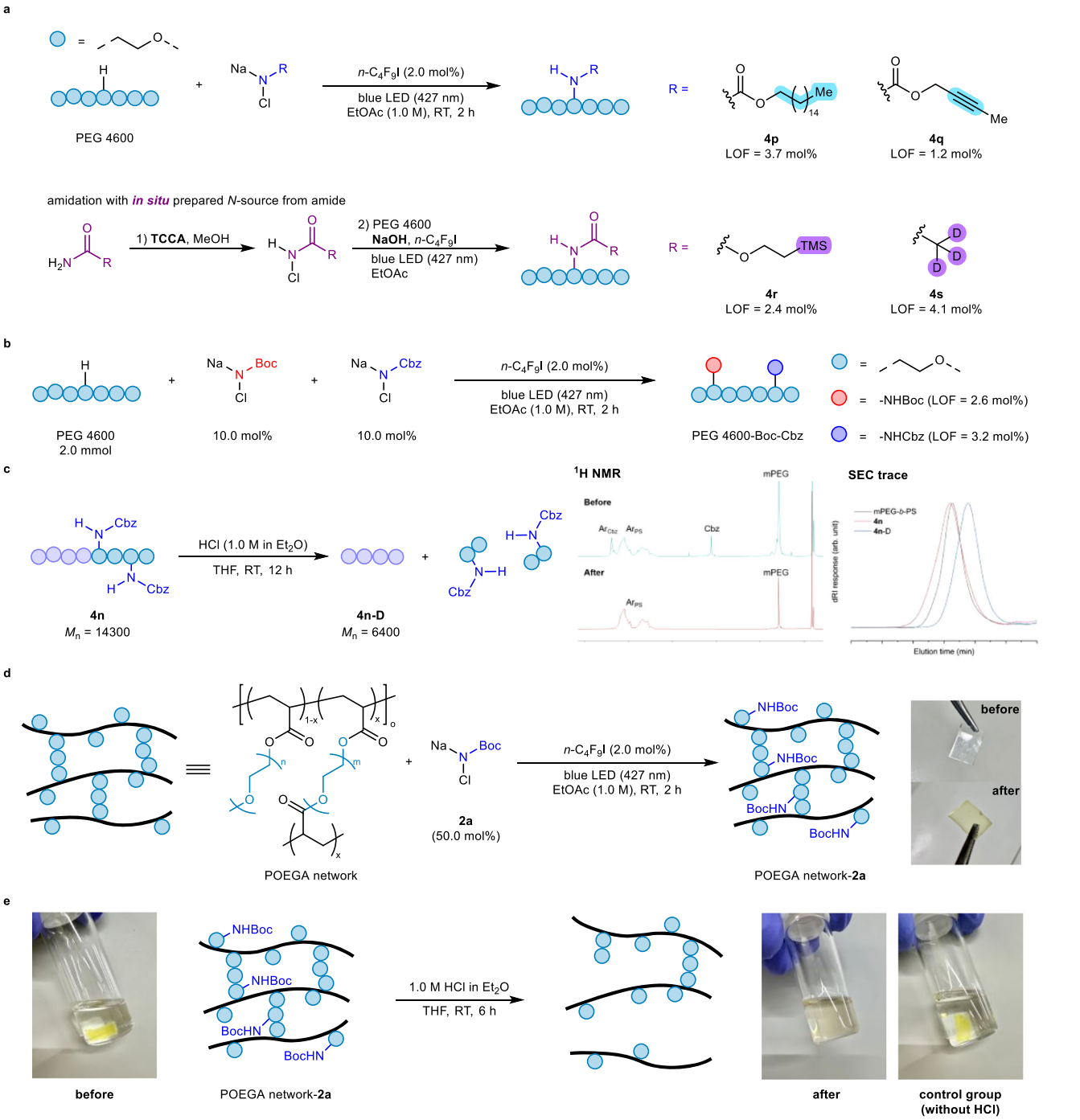

Fig. 6 | Access to functional polymeric materials with degradable features. **a** Functionalization of PEG incorporating different amide functionality: Reactions were carried out on 1.0 or 2.0 mmol scale based on the PEG repeating unit, using the corresponding *N*-chloro-*N*-sodio-carbamate (10.0 mol% for **4p**, 40.0 mol% for **4q**) or *N*-chloroamide (40.0 mol% for **4r**, 20.0 mol% for **4s**). **b** Double functionalization of PEG. **c** Degradation study of functionalized mPEG-*b*-PS. **d** Functionalization of cross-linked POEGA film. The yellow color comes from the installed amide groups. **e** Degradation of the amidated POEGA film. Note that the control group in neat THF retains the swollen state with the yellow color, indicating that the amide groups are intact.

ambient conditions, the presence of the acid-labile *N,O*-acetal group offers on-demand degradability. Unlike the current decomposition methods, which often require high temperatures or harsh conditions[71,72], these polyethers readily degrade under mild acidic conditions. For example, treating **4n** with 1.0 M HCl solution in diethyl ether at room temperature completely decomposed the PEG chain functionalized with -NHCbz, and recovered the PS block unchanged (Fig. 6c) (See Supplementary Information for details).

Interestingly, the photoinduced amidation reaction worked for cross-linked polymeric materials in the solvent-swollen state. We demonstrated this possibility with a PEG-based poly(oligo(ethylene glycol) acrylate) (POEGA) film, which is widely used as hydrogel scaffolds[73] and electrolytes[74] (Fig. 6d). The cross-linked network consisted of oligo(ethylene glycol) pendants and junctions tethered to the polymeric hydrocarbon strands. Swelling the film in the reactant solution in EtOAc and photoirradiation resulted in a free-standing film possessing α-amino ether groups as evidenced by FTIR, while retaining

the original dimensions after solvent evaporation. As the network junction is made of the ether linkage, the functionalized material was also degradable under acidic conditions (Fig. 6e).

Discussion

In summary, we have revealed a post-functionalization method for polyethers via a photoinduced α-amidation reaction, using a robust and practical carbamate amidating reagent. This process selectively forms new C–N bonds at the ethereal α-C–H bonds of small molecules and polymers through a polar-radical relay pathway. This represents the first example of direct nitrogen incorporation onto the polyether backbone and one of the few instances of non-degradable PEG post-modification. We propose that in situ generated ethereal α-carbo-radical is rapidly trapped, forming an α-chloro ether intermediate while preventing undesired chain scission or inter-chain coupling. Even small amounts of the installed amide group were shown to significantly alter physical properties of PEG, offering a means to control thermal properties by adjusting the degree of C–N bond incorporation. Material applications of current strategy were also examined, such as degradable features or modification of polymer network.

Methods

General procedure for the α-amidation of polyethers

In a glovebox, to an oven-dried reaction vial equipped with stir bar were added polyethers (2.0 mmol of repeating unit), amidating reagent (0.2 mmol), and anhydrous EtOAc (2.0 mL) under N_2 atmosphere. To the vial was added *n*-C_4F_9I (2.0 mol%). The vial was sealed, removed from the glovebox, and placed on a stirrer plate. The reaction mixture was vigorously stirred for 2 h with irradiation of blue LED (427 nm) by using Kessil Lamps. The reaction mixture was then filtered, concentrated, and purified by precipitation using CH_2Cl_2 and Et_2O. When necessary, product was dialyzed using a regenerated cellulose membrane in the acetone.

Data availability

The data that support the findings of this study are available within the paper and its Supplementary Information files (experimental procedures and characterization data), or from the corresponding author upon request. Crystallographic data for the structures reported in this paper have been deposited at the Cambridge Crystallographic Data Centre (CCDC), under deposition numbers CCDC 2418625 (**3i**), 2418626 (**3 l**), 2418627 (**3ta**). Copies of the data can be obtained free of charge via https://www.ccdc.cam.ac.uk/structures/ (or from Cambridge Crystallographic Data Centre, 12 Union Road, Cambridge, CB2 1EZ, United Kingdom; fax: +44-1223- 336-033; email: deposit@ccdc.cam.ac.uk). Cartesian coordinates of computationally optimized geometries are available in Supplementary Data 1.

References

1. Iha, R. K. et al. Applications of orthogonal "click" chemistries in the synthesis of functional soft materials. *Chem. Rev.* **109**, 5620–5686 (2009).
2. Franssen, N. M., Reek, J. N. & de Bruin, B. Synthesis of functional 'polyolefins': state of the art and remaining challenges. *Chem. Soc. Rev.* **42**, 5809–5832 (2013).
3. Blasco, E., Sims, M. B., Goldmann, A. S., Sumerlin, B. S. & Barner-Kowollik, C. 50th anniversary perspective: polymer functionalization. *Macromolecules* **50**, 5215–5252 (2017).
4. Nakamura, Y. et al. Controlled radical polymerization of ethylene using organotellurium compounds. *Angew. Chem. Int. Ed.* **57**, 305–309 (2018).
5. Tan, C. & Chen, C. Emerging palladium and nickel catalysts for copolymerization of olefins with polar monomers. *Angew. Chem. Int. Ed.* **58**, 7192–7200 (2019).
6. Gauthier, M. A., Gibson, M. I. & Klok, H. A. Synthesis of functional polymers by post-polymerization modification. *Angew. Chem. Int. Ed.* **48**, 48–58 (2009).
7. Boaen, N. K. & Hillmyer, M. A. Post-polymerization functionalization of polyolefins. *Chem. Soc. Rev.* **34**, 267–275 (2005).
8. Yang, Y., Nishiura, M., Wang, H. & Hou, Z. Metal-catalyzed C–H activation for polymer synthesis and functionalization. *Coord. Chem. Rev.* **376**, 506–532 (2018).
9. Williamson, J. B., Lewis, S. E., Johnson, R. R. 3rd, Manning, I. M. & Leibfarth, F. A. C–H functionalization of commodity polymers. *Angew. Chem. Int. Ed.* **58**, 8654–8668 (2019).
10. Fazekas, T. J. et al. Diversification of aliphatic C–H bonds in small molecules and polyolefins through radical chain transfer. *Science* **375**, 545–550 (2022).
11. Ciccia, N. R. et al. Diverse functional polyethylenes by catalytic amination. *Science* **381**, 1433–1440 (2023).
12. Bae, C. et al. Catalytic hydroxylation of polypropylenes. *J. Am. Chem. Soc.* **127**, 767–776 (2005).
13. Williamson, J. B. et al. Chemo- and regioselective functionalization of isotactic polypropylene: a mechanistic and structure-property study. *J. Am. Chem. Soc.* **141**, 12815–12823 (2019).
14. Shin, J. et al. Controlled functionalization of crystalline polystyrenes via activation of aromatic C–H bonds. *Macromolecules* **40**, 8600–8608 (2007).
15. Lewis, S. E., Wilhelmy, B. E. & Leibfarth, F. A. Upcycling aromatic polymers through C–H fluoroalkylation. *Chem. Sci.* **10**, 6270–6277 (2019).
16. Zhang, Z. et al. In-situ noncovalent interaction of ammonium ion enabled C–H bond functionalization of polyethylene glycols. *Nat. Commun.* **15**, 4445 (2024).
17. Zhang, Z. et al. Controllable C–H alkylation of polyethers via iron photocatalysis. *J. Am. Chem. Soc.* **145**, 7612–7620 (2023).
18. Kim, S. J. et al. C–H functionalization of poly(ethylene oxide) – embracing functionality, degradability, and molecular delivery. *Macromol. Rapid. Commun.* **46**, 2400613 (2025).
19. Wencel-Delord, J. & Glorius, F. C–H bond activation enables the rapid construction and late-stage diversification of functional molecules. *Nat. Chem.* **5**, 369–375 (2013).
20. Davies, H. M. L. & Morton, D. Collective approach to advancing C–H functionalization. *ACS Cent. Sci.* **3**, 936–943 (2017).
21. Monfardini, C. & Veronese, F. Stabilization of substances in circulation. *Bioconjugate Chem.* **9**, 418–450 (1998).
22. Roverts, M. J., Bentley, M. D. & Harris, J. M. Chemistry for peptide and protein PEGylation. *Adv. Drug Deliv. Rev.* **54**, 459–476 (2002).
23. Turecek, P. L., Bossard, M. J., Schoetens, F. & Ivens, I. A. PEGylation of biopharmaceuticals: a review of chemistry and nonclinical safety information of approved drugs. *J. Pharm. Sci.* **105**, 460–475 (2016).
24. Lin, C.-C. & Anseth, K. S. PEG hydrogels for the controlled release of biomolecules in regenerative medicine. *Pharm. Res.* **26**, 631–643 (2008).
25. Fenton, D. E., Parker, J. M. & Wright, P. V. Complexes of alkali metal ions with poly(ethylene oxide). *Polymer* **14**, 589 (1973).
26. Zhou, D., Shanmukaraj, D., Tkacheva, A., Armand, M. & Wang, G. Polymer electrolytes for lithium-based batteries: advances and prospects. *Chem* **5**, 2326–2352 (2019).
27. Xu, S. et al. Homogeneous and fast ion conduction of PEO-based solid-state electrolyte at low temperature. *Adv. Funct. Mater.* **30**, 2007172 (2020).
28. Lee, J. & Kim, B. S. Recent progress in poly(ethylene oxide)-based solid-state electrolytes for lithium-ion batteries. *Bull. Korean Chem. Soc.* **44**, 831–840 (2023).
29. Obermeier, B., Wurm, F., Mangold, C. & Frey, H. Multifunctional poly(ethylene glycol)s. *Angew. Chem. Int. Ed.* **50**, 7988–7997 (2011).
30. Verkoyen, P. & Frey, H. Amino-functional polyethers: versatile, stimuli-responsive polymers. *Polym. Chem.* **11**, 3940–3950 (2020).

31. Fournier, D., Hoogenboom, R. & Schubert, U. S. Clicking polymers: a straightforward approach to novel macromolecular architectures. *Chem. Soc. Rev.* **36**, 1369–1380 (2007).
32. Wu, W. & Parent, J. S. Polymer functionalization by free radical addition to alkynes. *J. Polym. Sci. Part A* **46**, 7386–7394 (2008).
33. Reid, B., Tzeng, S., Warren, A., Kozielski, K. & Elisseeff, J. Development of a PEG derivative containing hydrolytically degradable hemiacetals. *Macromolecules* **43**, 9588–9590 (2010).
34. Liu, D. & Bielawski, C. W. Synthesis of degradable poly[(ethylene glycol)-co-(glycolic acid)] via the post-polymerization oxyfunctionalization of poly(ethylene glycol). *Macromol. Rapid. Commun.* **37**, 1587–1592 (2016).
35. Dian, L., Xing, Q., Zhang-Negrerie, D. & Du, Y. Direct functionalization of alkyl ethers to construct hemiaminal ether skeletons (HESs). *Org. Biomol. Chem.* **16**, 4384–4398 (2018).
36. Huard, K. & Lebel, H. *N*-tosyloxycarbamates as reagents in rhodium-catalyzed C–H amination reactions. *Chem. Eur. J.* **14**, 6222–6230 (2008).
37. Lebel, H. & Huard, K. De novo synthesis of Troc-protected amines: intermolecular rhodium-catalyzed C–H amination with *N*-tosyloxycarbamates. *Org. Lett.* **9**, 639–642 (2007).
38. Du, Y. D., Xu, Z. J., Zhou, C. Y. & Che, C. M. An effective [Fe^{III}(TF_4DMAP)Cl] catalyst for C–H bond amination with aryl and alkyl azides. *Org. Lett.* **21**, 895–899 (2019).
39. Hernandez-Guerra, D. et al. Photochemical C–H amination of ethers and geminal difunctionalization reactions in one pot. *Angew. Chem. Int. Ed.* **58**, 12440–12445 (2019).
40. Chen, J., Wang, H., Day, C. S. & Martin, R. Nickel-catalyzed site-selective intermolecular C(sp^3)–H amidation. *Angew. Chem. Int. Ed.* **61**, e202212983 (2022).
41. Lee, W. et al. Controlled relay process to access N-centered radicals for catalyst-free amidation of aldehydes under visible light. *Chem* **7**, 495–508 (2021).
42. Lee, W., Kim, D., Seo, S. & Chang, S. Photoinduced α-C–H amination of cyclic amine scaffolds enabled by polar-radical relay. *Angew. Chem. Int. Ed.* **61**, e202202971 (2022).
43. Jeon, H. J., Lee, W., Seo, S. & Chang, S. *N*-Chloro-*N*-sodio-carbamates as a practical amidating reagent for scalable and sustainable amidation of aldehydes under visible light. *Org. Process Res. Dev.* **25**, 1176–1183 (2021).
44. Nayak, Y. N. et al. Chloramine-T (*N*-chloro-p-toluenesulfonamide sodium salt), a versatile reagent in organic synthesis and analytical chemistry: An up to date review. *J. Saudi Chem. Soc.* **26**, 101416 (2022).
45. Campbell, M. M. & Johnson, G. Chloramine T and related *N*-halogeno-*N*-metallo reagents. *Chem. Rev.* **78**, 65–79 (2002).
46. Lee, J., McGrath, A. J., Hawker, C. J. & Kim, B. S. pH-tunable thermoresponsive PEO-based functional polymers with pendant amine groups. *ACS Macro Lett.* **5**, 1391–1396 (2016).
47. Shukla, G. & Ferrier, R. C. The versatile, functional polyether, polyepichlorohydrin: history, synthesis, and applications. *J. Polym. Sci.* **59**, 2704–2718 (2021).
48. Tagami, K., Ofuji, Y., Kanbara, T. & Yajima, T. Metal-free visible-light-induced hydroxy-perfluoroalkylation of conjugated olefins using enamine catalyst. *RSC Adv.* **12**, 32790–32795 (2022).
49. Wang, Y., Wang, J., Li, G. X., He, G. & Chen, G. Halogen-bond-promoted photoactivation of perfluoroalkyl iodides: a photochemical protocol for perfluoroalkylation reactions. *Org. Lett.* **19**, 1442–1445 (2017).
50. Sun, X., Wang, W., Li, Y., Ma, J. & Yu, S. Halogen-bond-promoted double radical isocyanide insertion under visible-light irradiation: synthesis of 2-fluoroalkylated quinoxalines. *Org. Lett.* **18**, 4638–4641 (2016).
51. Pan, Z., Fan, Z., Lu, B. & Cheng, J. Halogen-bond-promoted α-C–H amination of ethers for the synthesis of hemiaminal ethers. *Adv. Synth. Catal.* **360**, 1761–1767 (2018).
52. Wang, Y. et al. Activation of perfluoroalkyl iodides by anions: extending the scope of halogen bond activation to C(sp^3)–H amidation, C(sp^2)–H iodination, and perfluoroalkylation reactions. *Chem. Sci.* **14**, 1732–1741 (2023).
53. Roy, S. & Chatterjee, I. Visible-light-mediated (sp^3)Cα–H functionalization of ethers enabled by electron donor–acceptor complex. *ACS Org. Inorg. Au* **2**, 306–311 (2022).
54. Campos, J., Goforth, S. K., Crabtree, R. H. & Gunnoe, T. B. Metal-free amidation of ether sp^3 C–H bonds with sulfonamides using $PhI(OAc)_2$. *RSC Adv.* **4**, 47951–47957 (2014).
55. Studer, A. & Vogler, T. Applications of TEMPO in synthesis. *Synthesis* **2008**, 1979–1993 (2008).
56. Xie, W., Yoon, J. H. & Chang, S. (NHC)Cu-catalyzed mild C–H amidation of (hetero)arenes with deprotectable carbamates: scope and mechanistic studies. *J. Am. Chem. Soc.* **138**, 12605–12614 (2016).
57. Alfonsi, K. et al. Green chemistry tools to influence a medicinal chemistry and research chemistry based organisation. *Green. Chem.* **10**, 31–36 (2008).
58. Imbrogno, J. et al. Relationship between ionic conductivity, glass transition temperature, and dielectric constant in poly(vinyl ether) lithium electrolytes. *ACS Macro. Lett.* **10**, 1002–1007 (2021).
59. Naboulsi, A. et al. Correlation between Ionic Conductivity and Mechanical Properties of Solid-like PEO-based Polymer Electrolyte. *ACS Appl. Mater. Interfaces* **16**, 13869–13881 (2024).
60. Kelly, I. E., Owen, J. R. & Steele, B. C. H. Poly(ethylene oxide) electrolytes for operation at near room temperature. *J. Power Sources* **14**, 13–21 (1985).
61. Ebagninin, K. W., Benchabane, A. & Bekkour, K. Rheological characterization of poly(ethylene oxide) solutions of different molecular weights. *J. Colloid Interface Sci.* **336**, 360–367 (2009).
62. Park, H. & Wang, Q. State-of-the-art accounts of hyperpolarized ^{15}N-labeled molecular imaging probes for magnetic resonance spectroscopy and imaging. *Chem. Sci.* **13**, 7378–7391 (2022).
63. Kim, H.-C., Park, S.-M. & Hinsberg, W. D. Block copolymer based nanostructures: materials, processes, and applications to electronics. *Chem. Rev.* **110**, 146–177 (2009).
64. Gaucher, G. et al. Block copolymer micelles: preparation, characterization and application in drug delivery. *J. Controlled Rel.***109**, 169–188 (2005).
65. Lazzari, M., Liu, G. & Lecommandoux, S. B. *Block copolymers in nanoscience* (Wiley-VCH, 2006).
66. Bates, F. S. & Fredrickson, G. H. Block copolymers—designer soft materials. *Phys. Today* **52**, 32–38 (1999).
67. Abetz, V. & Simon, P. F. W. in *Block Copolymers I* (ed. Volker Abetz) 125–212 (Springer, 2005).
68. Karayianni, M. & Pispas, S. Block copolymer solution self-assembly: recent advances, emerging trends, and applications. *J. Polym. Sci.* **59**, 1874–1898 (2021).
69. Jeong, B., Bae, Y. H., Lee, D. S. & Kim, S. W. Biodegradable block copolymers as injectable drug-delivery systems. *Nature* **388**, 860–862 (1997).
70. Cho, H., Gao, J. & Kwon, G. S. PEG-*b*-PLA micelles and PLGA-*b*-PEG-*b*-PLGA sol–gels for drug delivery. *J. Controlled Rel.* **240**, 191–201 (2016).
71. Mao, H. & Hillmyer, M. A. Nanoporous polystyrene by chemical etching of poly(ethylene oxide) from ordered block copolymers. *Macromolecules* **38**, 4038–4039 (2005).
72. Raghuvir, P. B., Kulkarni, A., Dasari, H. & Mathew, T. M. Current status of methods used in degradation of polymers: a review. *MATEC Web Conf.* **144**, 02023 (2018).

73. Vancoillie, G., Frank, D. & Hoogenboom, R. Thermoresponsive poly(oligo ethylene glycol acrylates). *Prog. Polym. Sci.* **39**, 1074–1095 (2014).
74. Xue, Z., He, D. & Xie, X. Poly(ethylene oxide)-based electrolytes for lithium-ion batteries. *J. Mater. Chem. A* **3**, 19218–19253 (2015).

Acknowledgements

This research was supported by the Institute for Basic Science (IBS-R010-D1, S.C.) in South Korea, National Research Foundation of Korea (NRF) grant funded by the Korea government (MSIT) (2018R1A5A1025208 and 2023R1A2C2005705, M.S.), and the Ministry of Trade, Industry and Energy through the Bio-Industrial Technology Development Program (20008628, M.S.). Computational works for this research were performed on the High Performance Computing Resources in the IBS Research Solution Center.

Author contributions

S.C. and M.S. conceived and designed the project. S.B.B. and Y.K. carried out all experiments, including reaction optimization, scope investigation and mechanistic studies. S.B.B. also performed density functional theory (DFT) calculations. W.L. and S.S. assisted in experimental design. D.K. performed the X-ray crystallographic analysis. All authors contributed to the manuscript preparation, as well as the analysis and interpretation of the results.

Competing interests

The authors declare no competing interests.

Additional information

Supplementary information The online version contains supplementary material available at https://doi.org/10.1038/s41467-025-63254-z.

Correspondence and requests for materials should be addressed to Myungeun Seo or Sukbok Chang.

Peer review information *Nature Communications* thanks the anonymous reviewers for their contribution to the peer review of this work. A peer review file is available.